Ultrawideband axion search using a Faraday haloscope

A. T. M. Anishur Rahman*

Department of Physics, University of Warwick, Coventry CV4 7AL, United Kingdom

(Received 31 July 2022; accepted 28 November 2022; published 19 December 2022)

Dark matter is a major constituent of our Universe and the axion is a prime candidate. In this article, it is shown that by exploiting the axion induced magnetization in a magnetic rod and the Faraday effect, axions in the mass range 500–5000 μeV, a part of which (> 3500 μeV) is currently inaccessible to experiments, can be searched for using the same experimental setup in a year using the existing technologies. The magnetic rod is placed inside a high-finesse optical cavity, which by confining the probe light inside it increases the interaction time and thus enhances the Faraday effect. This rotates the plane of polarization of the probe light sufficiently and produces a robust signal. Axions of different mass are selected using a dc magnetic field. Detection is carried out by counting photons in the optical domain using a readily available and high quantum efficiency (≈1) photon counter in a noise-free environment. An optical interferometric scheme that could provide spectroscopic information about the axion to be searched is also proposed.

DOI: 10.1103/PhysRevD.106.115017

The strong interactions, in violation to the standard model of particle physics, conserve parity (P) and the product CP of charge (C) and parity [1]. To solve these inconsistencies, Peccei and Quinn proposed a scalar field and a pseudoparticle called the axion [2]. Considering the Planck scale the lower bound of axion mass has been found to be 10^{-13} eV while the upper bound of 10^{-2} eV has been determined from the consideration of stellar evolution [1]. Cold axions produced via the vacuum realignment process are good dark matter candidates [3–5] and may be the main constituent of the dark matter at 10^{-5} eV [1,6]. However, there are substantial uncertainties—approximately four orders of magnitude, arising from the uncertainty in the composition of the dark matter, their densities and the temperature [1]. Significant uncertainties also exist in the velocity and the equilibrium state of the Galactic halo [1]—the main axionic source of most proposed and current experiments [6–13]. These theoretical uncertainties mean that experimental searches for detecting such particles need to be wideband [1,6,7].

Major experimental efforts center around converting axions into microwave photons inside a microwave cavity in a strong magnetic field [7–9]. Over the decades such experiments have ruled out axions between 2.7–4.2 μeV and can search axions of masses up to few tens of μeV [1,7–9]. Another class of experiments exploits the axion-electron interaction in a ferromagnetic material placed inside a microwave cavity [6,10,11,14] and converts axions into microwave photons. Due to the resonant nature of the microwave-cavity based schemes [7–9,11,15], searching axions of substantially different mass than the resonance frequencies of such cavities requires a new cavity implying a prolonged time (decades) for scanning the axion spectrum. Moreover, in most proposed and current axion experiments [7–11,13], detection is accomplished by measuring the microwave power produced in the axion to microwave conversion process. Such a conversion yields an extremely small amount of power ($< 10^{-20}$ W) requiring multistage amplifications which are often plagued by the dominant electronic noise [7,9,11,15]. Here, more sensitive detectors such as photon counters are highly desirable [1,11,15,16] but are not readily available in the microwave domain.

In this article we propose an axion search scheme in which the axion-electron interaction initiates oscillation in magnetization in a magnetic rod and a linearly polarized probe light traveling through the sample interacts with this oscillatory magnetization via the Faraday effect and converts microwave frequency axions into optical photons. The magnetic rod is placed inside a high-finesse optical cavity which by trapping the probe light for a prolonged period of time greatly increases the interaction time and thus enhances the Faraday effect. On exiting the optical cavity, the plane of polarization of the probe light gets rotated and this produces a signal proportional to the light field power. The signal in the optical domain means that readily available photon counters can be used. The axion to be searched for is selected by adjusting the dc bias magnetic field. Importantly, since the Faraday effect only changes the plane of polarization of the light field, the optical cavity remains on resonance when the magnetic field is changed for searching axions of different mass. This means that axions in the mass range 500–5000 μeV can be searched

*anishur.rahman@warwick.ac.uk

for using the same experimental setup in the time scale of a year. Axion mass > 3500 μeV is currently inaccessible to experiments.

In the nonrelativistic limit, the axion-electron interaction is given by [1,6]

$$H_{ae} = \frac{g_{ae}}{f_a} \nabla a \cdot \mathbf{S}, \tag{1}$$

where $\mathbf{S}$ is the spin of the magnetic system, f_a is the axion decay constant and a is the scalar axionic field. The axion-electron coupling strength is given by g_{ae} and in the Dine-Fischler-Srednicki-Zhitnisky (DFSZ) model [17,18] is proportional to the axionic mass m_a i.e., $g_{ae} \approx 3 \times (m_a/1\ \text{eV})$. Equation (1) can be remodeled as a spin system in a magnetic field e.g., $\mathbf{B_a} \cdot \mathbf{S}$, where $\mathbf{B_a} = \frac{g_{ae}}{f_a} \nabla a$. The effective axionic magnetic field [1,6,19] along the x axis is $B_{a_x} = B^0_{a_x} \sin \omega_a t$, where $B^0_{a_x} = \frac{g_{ae}}{2q_e} \sqrt{\frac{n_a \hbar m_a}{c}} v_x$, c is the speed of light in vacuum, $\hbar$ is the Planck constant, q_e is the electronic charge, $n_a \approx 3 \times 10^8 (1\ \text{eV}/m_a)$ is the axion dark matter density, $v_x = v_a[b_0 \cos(\lambda_{\text{lab}}) - b_1 \sin(\lambda_{\text{lab}}) \cos(\omega_d t + \phi_{\text{lab}} + \psi)]$ with $\omega_d = 2\pi/T_d$ and $T_d \approx 84600$ s. The speed of axion v_a in the laboratory frame varies between 220 km/s and 250 km/s in a period equal to a year [19]. Parameters b_0, b_1, and ψ vary over the year and depend on v_a [19]. The latitude and the longitude of the Earth-bound laboratory are denoted by λ_{lab} and ϕ_{lab}, respectively.

Consider a ferromagnetic rod of length L and radius r is immersed in the axionic magnetic field B_{a_x} and placed inside an optical cavity in a cryogenic environment. The cavity can be formed by using two identical high-reflectivity mirrors as shown in Fig. 1 or by appropriately coating all surfaces of the rod with antireflection coatings. Using the rod itself as a cavity can potentially render a simpler and more stable experimental setup. The rod is illuminated with a linearly polarized (along z-axis) probe light propagating along the cavity axis (y-axis, Fig. 1). The radius of the laser beam is r. The rod is magnetized to saturation using a dc magnetic field B_0 applied along the z axis. An oscillating magnetic field, here the axionic field B_{a_x}, in the x–y plane initiates a precession of the magnetic moment around B_0. The frequency of the precession $\omega_a \approx m_a c^2/\hbar$ and thus the mass of the dark matter to be detected is determined by the magnitude of B_0 via $\omega_a/2\pi = \gamma B_0$. For a rod, the ferromagnetic resonance frequency is slightly different than γB_0 due to the shape related demagnetization [20]. In the following, however, we do not consider this effect for the analytical simplicity. Precession of the magnetic moment around the z-axis means that a component of the magnetic moment appears in the x–y plane. This component of the magnetic moment oscillates at ω_a and is known as the uniform precession mode or the Kittel mode.

The induced magnetic moment in the x–y plane can be found by solving the Bloch equation [20]

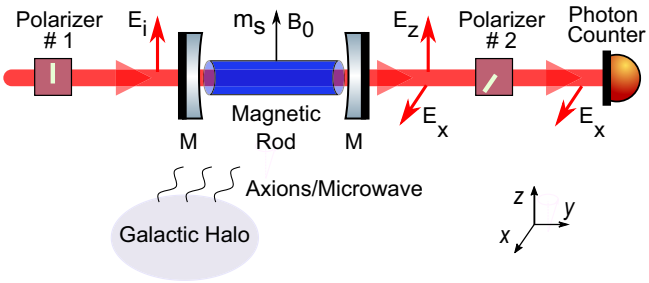

FIG. 1. A schematic diagram of the proposed experimental setup. A magnetic rod biased to the saturation using a dc magnetic B_0 applied along the z-axis is placed inside a high finesse optical cavity. The cavity is formed by the two mirrors (M). Axions from the Galactic halos acting as an electromagnetic field and arriving along the x-axis couples to the electronic spin in the rod. This initiates precession of the spins or a magnetization and a component of magnetization appears in the x–y plane i.e., m_y. Linearly polarized (z-axis) light propagating along the y axis interacts with the induced magnetization m_y via the Faraday effect and on exiting the cavity its plane of polarization gets rotated. Polarizer #2 picks up the x component of the light field. The axes of polarizers 1 and 2 are orthogonal to each other. The x component of the light field is the axionic signal and detected using a photon counter (see text for more details).

$\frac{d\mathbf{m}}{dt} = \gamma(\mathbf{m} \times \mathbf{B}) - \mathbf{m}/T_{1,2}$, where $\mathbf{m}$ is the magnetic moment of the rod, γ is the gyromagnetic ratio, and $\mathbf{B} = B_{a_x}\hat{x} + B_0\hat{z}$. The spin-lattice and the spin-spin relaxation time are denoted by T_1 and T_2, respectively. Given B_{a_x} is expected to be many orders of magnitude smaller than B_0 ($B_{a_x} \ll B_0$) [10], we have $(m_x, m_y) \ll m_z$. This allows us to set $m_z \approx m_s$ and $\frac{dm_z}{dt} \approx 0$, where m_s is the saturation magnetic moment of the rod. In the steady state the y component of the induced magnetic moment is

$$m_y = \frac{m_s \gamma T_2}{2} B^0_{a_x} \sin \omega_a t. \tag{2}$$

Linearly polarized light $\mathbf{E}_i = E_i \hat{z}$ propagating along the cavity axis (y axis) interacts with m_y via the Faraday effect and its plane of polarization rotates by an angle $\frac{V_r L m_y}{m_s}$ [21–23], where $E_i = \sqrt{2I_i/(\epsilon_0 c)}$, ϵ_0 is the permittivity of free space, $I_i = \frac{P}{\pi r^2}$ is the intensity of the input laser light to the cavity, P is the input optical power, and V_r is the Verdet constant of the rod in radian per meter. The direction of the light field propagation is denoted by $\mathbf{k} = k\hat{y}$. To ensure that light of the purest polarization state enters the cavity, it is filtered using a polarizer of adequate extinction ratio. In principle, a polarizer of an arbitrarily high extinction ratio can be engineered by using multiple metamaterial polarizers in cascade [24,25]. In an optical isolator, also known as the Faraday rotator, the saturation magnetization $\mathbf{m_s}$ and the direction of the light field propagation are parallel and there is no magnetization orthogonal to $\mathbf{m_s}$ hence the

rotation angle is $V_r L$ [21]. In our case, since only a fraction of the magnetization is parallel to $\mathbf{k}$, the rotation angle is reduced by the factor $\frac{m_y}{ms}$ [21,22]. The presence of the optical cavity means that light bounces back and forth between the mirrors for $N = \tau_c/\tau$ times before exiting the cavity [26], where $\tau_c = \frac{n_c L_c}{c(1-R_c)}$ is the photon lifetime in the cavity and $\tau = n_c L_c/c$ is the time required by the light to go from one mirror of the cavity to the other, n_c is the refractive index of the cavity filler material, L_c is the length of the cavity and R_c is the reflectivity of the cavity mirrors. This means that the light interacts with m_y N times. Due to the nonreciprocal nature of the Faraday effect [21,23], each time light interacts with m_y, its plane of polarization is rotated by another $\frac{V_r L m_y}{m_s}$ radians. On exiting the cavity, the plane of polarization of the light field is rotated by an angle $\theta_f = \frac{N V_r m_y L}{m_s}$. In an ideal lossless cavity, the electric field after the cavity is $\mathbf{E}_o = E_i \sin\theta_f \hat{x} + E_i \cos\theta_f \hat{z}$. The x component (E_x) of $\mathbf{E}_o$ is picked up using a polarizer (Fig. 1) and is the desired signal. The optical power $P_x = \pi r^2 \epsilon_0 c \langle E_x^2 \rangle$ is

$$P_x = P\sin^2\theta_f \approx \frac{P V_r^2 L^2 \gamma^2 T_2^2}{4(1-R_c)^2}(B^0_{a_x}\sin\omega_a t)^2, \qquad (3)$$

where we have set $\sin\theta_f \approx \theta_f$ as θ_f is expected to be $\ll 1°$ (see below). Equation (3) shows that P_x is subjected to the daily and the yearly modulation via the axionic field B_{a_x}, a unique signature of the axion dark matter. Most importantly, however, axions of any mass, at least in principle, can be searched by merely adjusting the dc magnetic field ($\omega_a/2\pi = \gamma B_0$) without changing any component of the proposed experiment. This is possible as axions of different masses only change the plane of polarization of the light field. Consequently, the optical cavity remains on resonance with the laser when B_0 is changed. Since B_0 can be controlled by changing the current through the magnet, no component in the setup needs to be modified for searching different axions. Hence the whole axion spectrum within the sensitivity of the Faraday haloscope can be searched using the same setup in a relatively short time (see below). The axion induced signal P_x can be enhanced using a long rod, a higher optical power, a long spin-coherence time, and a magnetic material with a high Verdet constant. P_x can also be boosted by increasing $N = 1/(1-R_c)$ using ultrahigh reflectivity cavity mirrors provided $N\tau \leq T_2$. This implies that the preferable cavity length is $L_c = L$.

Detection is often the most challenging aspect of axion search experiments. Here, we accomplish this using a photon counter which is capable of detecting a single photon. High quantum efficiency (≈1) photon counters in the visible [27] and the infrared bands [28,29] are readily available. Indeed, it is a unique feature of the proposed experiment in that it converts axions into optical photons and then takes advantage of the high-efficiency photon counters available in the optical domain. Photon counters in the infrared band have dark counts, a potential source of noise, $\ll 1\ \mathrm{s}^{-1}$ [28,29]. As a result, detection can be accomplished free of noise which often, in existing experiments, dominates axionic signals [7,11,15]. The number of photons equivalent to P_x is $P_x\lambda/(hc)$, where λ is the wavelength of the laser light.

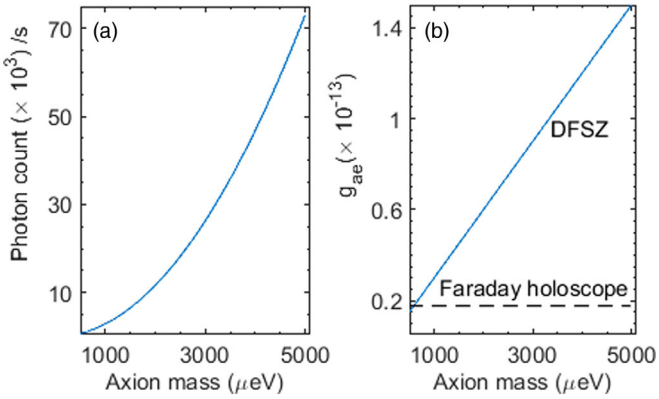

FIG. 2. (a) Assuming the DFSZ model of axion-electron coupling, the average number of photons detected as a function of axion mass at midnight on January 1 when a $r = 12.5$ mm and $L = 100$ mm cerium doped YIG rod is illuminated with 100 mW laser power. Other parameters are $R_c = 99.999\%$, $\lambda = 1550$ nm, $T_2 = 50$ μs, and $V_r = 1.75 \times 10^4$ rad/m. (b) Axion electron coupling strength g_{ae} as a function of axion mass in DFSZ model (solid line). The dashed line shows the minimum g_{ae} that the Faraday haloscope can operate with and produces at least 1000 photon counts (see the main text for detail).

Let us now consider an example. Here, a magnetic material with a high Verdet constant and a long-spin coherence time is desirable. Yttrium iron garnet (YIG) [22] and its variants such as cerium substituted YIG [30,31] might be good candidates. YIG is widely used in quantum magnonics [32] and science [33] for its long-spin coherence time. It has a moderate Verdet constant [22] and is often used as an optical isolator meaning that it can handle high-intensity lasers [30,34]. Substitution of yttrium by the nonmagnetic cerium (Ce) enhances the Faraday rotation of YIG significantly while maintaining the magnetic properties of the undoped YIG [31,34]. At cryogenic temperature, V_r of Ce:YIG increases rapidly and at 300 mK in a cryostat it can reach $\approx 1.75 \times 10^4$ rad/m [30]. Figure 2 shows the average number of photons as a function of axion mass when a $r = 12.5$ mm and $L = 100$ mm Ce:YIG rod is illuminated with 100 mW optical power at $\lambda = 1550$ nm. At this wavelength cerium doped YIG is transparent [34]. Lasers with extremely low-intensity and frequency noise, narrow linewidths (≈1 kHz), and high stability at 1550 nm are available [35,36]. The $\langle 111 \rangle$ crystalline axis of YIG is along the long axis of the rod. The strength of the required

magnetic field for scanning the axion mass range shown in Fig. 2(a) is between $B_0 = 4.3$ T and 42.85 T. Highly homogeneous superconducting magnets up to 28.2 T are commercially available [37] and a 45 T magnet is available as a national facility for decades [38,39]. At $m_a = 500$ μeV, the number of photons is $\approx 1 \times 10^3$/s while at 2000 μeV it is $\approx 12 \times 10^3$/s. These are significant and should be easily detectable using a 1550 nm photon counter [28,29]. Using a higher laser power, axions below 500 μeV can be searched. At 500 μeV, θ_f is 2.20×10^{-8} rad. In the calculations we have used the coordinates of the University of Warwick, $R_c = 99.999\%$ [40] and a spin coherence time of $T_2 = 50$ μs [20,41]. Note that $T_2 = 1/\Delta f$, where Δf is the full width half-maximum linewidth of a magnetic resonance peak [20].

To ensure that light polarized along the z-axis (Fig. 1) does not reach the detector, the polarizer in front of the photon counter must efficiently block the z-polarized light. In principle, a polarizer can have an arbitrarily high polarization extinction ratio γ_r [24,25]. The number of photons in the 1550 nm beam (100 mW) is $\approx 10^{18}$. To ensure that none of these photons enters the photon counter when no axion ($E_x = 0$) is present, $\gamma_r = 10^{20}$ is sufficient. To achieve this level of polarization extinction, up to eight dual grating metamaterial based polarizers may be required [24]. Importantly, light transmission through these polarizers is close to 100%. The relative intensity noise (RIN) which represents the combined effect of shot noise, $1/f$ noise, and beam-pointing instabilities can potentially cause performance degradation of the Faraday haloscope via fluctuation in the photon counts. However, highly-stable, low-intensity, and frequency noise, and narrow linewidth lasers are available [35,36]. When monitored for a prolonged period of time (≈2 weeks) such a laser showed virtually no drift [36]. This laser has a RIN ≤ -140 dB/Hz at frequencies ≥ 0 Hz. When integrated between dc and 1 MHz assuming a constant RIN of −140 dB/Hz, such a noise results in an intensity fluctuation and hence a fluctuation in the photon count of $< 0.1\%$. This is negligible. Furthermore, the effect of laser shot noise on the photon count can be reduced by using the amplitude squeezed light [42]. Performance degradation of the Faraday haloscope due to the dark count of the photon counter is also negligible as such a counter has a very low dark count e.g., 5.6×10^{-3} per second [29]. Unwanted photons produced by the thermal excitation of the Kittel magnon can also reduce the fidelity of the axion produced photon counts. Here, a high purity sample is essential so that a very little or no laser power is absorbed. Any residual heating due to laser and blackbody absorption by the rod should be actively mitigated by the cryogenics with a sufficient cooling power. Nevertheless, the magnetic moment along the y axis due to such potential stimuli at temperature T [20] is $m_y^{\text{th}} = \mu_B V D(\omega)/(e^{\hbar\omega_a/k_B T} - 1)$,

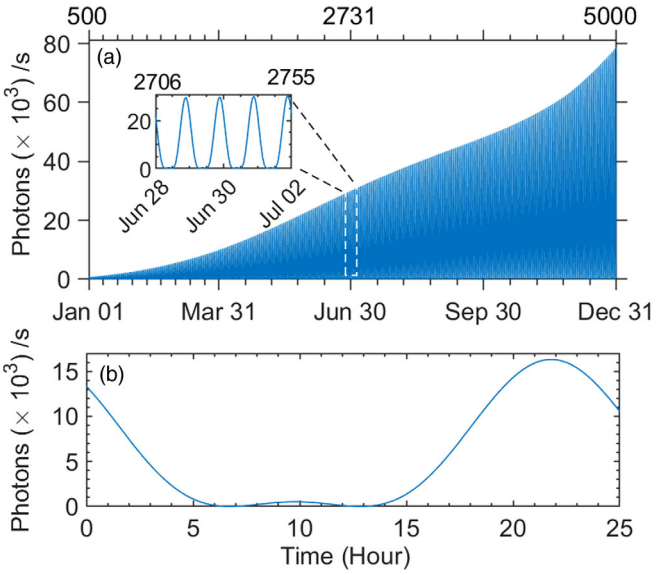

FIG. 3. (a) Photon counts when axions of different mass are searched for over a year. The top scale shows the axionic mass. The inset is the zoomed view when the search reaches 2731 μeV (June 30). (b) The predicted daily modulation of the number of photons counted over a day when the search is fixed at $m_a =$ 2000 μeV (May 02).

where μ_B is the Bohr magneton, $D(\omega_a) = (\frac{\hbar}{2JSa^2})^{3/2}\sqrt{\omega_a/16\pi^2}$ is the density of states of magnon at ω_a, J is the ferromagnetic exchange integral, a is the lattice constant and V is the volume of the rod. At $T =$ 300 mK and $m_a = 500$ μeV ($\omega_a/2\pi = 120$ GHz), we have $m_y^{\text{th}} = 1.63 \times 10^{-22}$ A/m. This is trivial compared to $\langle m_y \rangle = 5 \times 10^{-16}$ A/m [Eq. (2)]. Consequently, photon counts originating from thermal sources are not relevant.

Taking at least 1×10^3 photons per second (≫ the dark count) due to axion is a sufficiently strong signal, Fig. 2(b) shows the minimum axion-electron coupling strength that the Faraday haloscope can operate with. For comparison, this figure also shows g_{ae} expected from the DFSZ model. It is clear that the Faraday haloscope can produce enough photon counts even when the axion-electron coupling strength is smaller than that is predicted by the DFSZ model.

The rate at which axions can be searched for is critically important. In the proposed experiment, the magnetic field is the only parameter that needs to be changed for searching different axions and can be accomplished by changing the current through the magnet. Assuming twenty data points per day, each 0.6164 μeV apart, axions between 500 and 5000 μeV can be searched for in a year. Figure 3(a) shows the result of such a search starting on January 1 (500 μeV) and ending on December 31 (5000 μeV). Due to the daily and yearly motion of the earth through the dark matter halo, the photon count oscillates [(inset, Fig. 3(a)] as the search progresses. In particular, due to the earth's rotational

motion, irrespective of the axion mass, the signal goes to zero on daily basis at certain time of the day. This is captured in more detail in Fig. 3(b) where the search is fixed at 2000 μeV (May 02). It is clear that at around 10am the photon count is minimal while at around midnight the expected photon count peaks. Importantly, these periodic modulations mean that the proposed experiment, at least in principle, should be immune to any background count that may arise. In particular, due to the rotational and yearly motion of the earth the photon count arising from axions oscillates periodically (Fig. 3). In contrast, counts due to the background, on the average, should remain fixed and as such should appear as an offset in the measurement process.

As a complementary technique to photon counting, the anti-Stokes sideband associated with the Brillouin light scattering can be considered [43]. In this configuration, circularly polarized light is used and the optical cavity is avoided. The external magnetic field B_0 is applied along the y axis (Fig. 1). The axionic microwave field excites magnetization/magnons in the x–z plane. The interaction [43] between a Kittel magnon (zero linear momentum) and the circularly polarized light creates an anti-Stokes sideband at $\omega_l + \omega_a$, where $\omega_l = 2\pi\lambda/c$ is the angular frequency of the laser. The conservation of the angular momentum in the process of magnon (axion) to photon conversion is guaranteed via the rotational recoil in the crystal [43]. Also, since the light traveling through the Faraday active material interacts with the magnon only once, even a small T_2 can be sufficient as long as $T_2 > Ln_c/c$. This can be useful in using other materials with higher Verdet constants such as chromium tribromide [23]. Importantly, this detection scheme can provide spectroscopic information e.g., the frequency of the axion detected and its linewidth. The as-produced sideband interferes with a strong local oscillator at frequency ω_{lo} in a heterodyne scheme on a fast photodiode [43]. We have $[E_{lo}\cos\omega_{lo}t + E_s\cos(\omega_l + \omega_a)t]^2$, where E_s is the amplitude of the scattered light and $E_{lo}\cos\omega_{lo}t$ is the local oscillator field. The signal of interest is now $E_{lo}E_s\cos(\omega_l - \omega_{lo} + \omega_a)t$, where we have not shown the dc offset and the high frequency terms. As before, the frequency of axions to be detected is selected by adjusting the dc magnetic field (Fig. 1). A significant advantage of this interferometric detection is that a weak signal can be strengthened with a strong local oscillator. Given the availability of a low RIN (low-amplitude noise), highly-stable, narrow linewidth (≈1 kHz) and low-frequency/phase noise laser (e.g., 0.7 μrad/$\sqrt{\text{Hz}}$ at 1 kHz) [35,36], the heterodyne scheme proposed here is robust.

Finally, it is instructive to consider the sensitivity range of the Faraday haloscope and its place in the global axion search landscape. The cavity based search experiments such as the ADMX [7] and the QUAX [10,15] Collaborations can search axions up to few tens of μeV while the proposed MADMAX experiment [13] is sensitive between the axion mass 40 and 400 μeV. The proposed nuclear resonance [12] and the topological insulator [44] based schemes are sensitive to 1–1000 μeV and 700–3500 μeV, respectively. Here, the proposed Faraday haloscope can search axions between 500 μeV and 5000 μeV and is uniquely placed to expand the global axion search above 3500 μeV.

In conclusion, we have theoretically shown that axions of mass between 500 μeV and 5000 μeV can be searched for using a single experimental setup. In realizing the search scheme we have used the axion-induced rotation of the plane of polarization of the probe light field via the Faraday effect. Using an optical cavity has allowed us to amplify the weak Faraday effect significantly. We have also shown that a wideband search of axions over hundreds of μeV can be accomplished in the matter of a year. It has also been demonstrated that the detection can be accomplished using high quantum efficiency, well-developed and readily available photon counters in almost a noise-free environment. In the current article, we have considered cerium doped YIG as the Faraday active material which has a moderate Verdet constant. In contrast, chromium tribromide [23] has a significantly higher Verdet constant and can potentially be used instead of YIG. This can enhance the optical signal in a major way.

I acknowledge the comments and suggestions that I have received from G. Morley, C. Ghag, A. Pontin and Y. Ramachars which have improved the manuscript.

[1] P. Sikivie, Invisible axion search methods, Rev. Mod. Phys. **93**, 015004 (2021).
[2] R. D. Peccei and H. R. Quinn, *CP* Conservation in the Presence of Pseudoparticles, Phys. Rev. Lett. **38**, 1440 (1977).
[3] J. Preskill, M. B. Wise, and F. Wilczek, Cosmology of the invisible axion, Phys. Lett. **120B**, 127 (1983).
[4] M. Dine and W. Fischler, The not-so-harmless axion, Phys. Lett. **120B**, 137 (1983).
[5] L. Abbott and P. Sikivie, A cosmological bound on the invisible axion, Phys. Lett. **120B**, 133 (1983).
[6] R. Barbieri, C. Braggio, G. Carugno, C. Gallo, A. Lombardi, A. Ortolan, R. Pengo, G. Ruoso, and C. Speake, Searching

for galactic axions through magnetized media: The quax proposal, Phys. Dark Universe **15**, 135 (2017).
[7] C. Bartram *et al.* (ADMX Collaboration), Search for Invisible Axion Dark Matter in the 3.3–4.2 μeV Mass Range, Phys. Rev. Lett. **127**, 261803 (2021).
[8] N. Du *et al.* (ADMX Collaboration), Search for Invisible Axion Dark Matter with the Axion Dark Matter Experiment, Phys. Rev. Lett. **120**, 151301 (2018).
[9] S. J. Asztalos, G. Carosi, C. Hagmann, D. Kinion, K. van Bibber, M. Hotz, L. J. Rosenberg, G. Rybka, J. Hoskins, J. Hwang, P. Sikivie, D. B. Tanner, R. Bradley, and J. Clarke, Squid-Based Microwave Cavity Search for Dark-Matter Axions, Phys. Rev. Lett. **104**, 041301 (2010).
[10] D. Alesini, C. Braggio, G. Carugno, N. Crescini, D. D'Agostino, D. Di Gioacchino, R. Di Vora, P. Falferi, U. Gambardella, C. Gatti, G. Iannone, C. Ligi, A. Lombardi, G. Maccarrone, A. Ortolan, R. Pengo, A. Rettaroli, G. Ruoso, L. Taffarello, and S. Tocci, Search for invisible axion dark matter of mass $m_a = 43$ μeV with the quax–$a\gamma$ experiment, Phys. Rev. D **103**, 102004 (2021).
[11] G. Flower, J. Bourhill, M. Goryachev, and M. E. Tobar, Broadening frequency range of a ferromagnetic axion haloscope with strongly coupled cavity–magnon polaritons, Phys. Dark Universe **25**, 100306 (2019).
[12] A. Arvanitaki and A. A. Geraci, Resonantly Detecting Axion-Mediated Forces with Nuclear Magnetic Resonance, Phys. Rev. Lett. **113**, 161801 (2014).
[13] A. Caldwell, G. Dvali, B. Majorovits, A. Millar, G. Raffelt, J. Redondo, O. Reimann, F. Simon, and F. Steffen (MADMAX Working Group), Dielectric Haloscopes: A New Way to Detect Axion Dark Matter, Phys. Rev. Lett. **118**, 091801 (2017).
[14] R. Barbieri, M. Cerdonio, G. Fiorentini, and S. Vitale, Axion to magnon conversion. A scheme for the detection of galactic axions, Phys. Lett. B **226**, 357 (1989).
[15] N. Crescini, D. Alesini, C. Braggio, G. Carugno, D. D'Agostino, D. Di Gioacchino, P. Falferi, U. Gambardella, C. Gatti, G. Iannone, C. Ligi, A. Lombardi, A. Ortolan, R. Pengo, G. Ruoso, and L. Taffarello (QUAX Collaboration), Axion Search with a Quantum-Limited Ferromagnetic Haloscope, Phys. Rev. Lett. **124**, 171801 (2020).
[16] S. K. Lamoreaux, K. A. van Bibber, K. W. Lehnert, and G. Carosi, Analysis of single-photon and linear amplifier detectors for microwave cavity dark matter axion searches, Phys. Rev. D **88**, 035020 (2013).
[17] M. Dine, W. Fischler, and M. Srednicki, A simple solution to the strong cp problem with a harmless axion, Phys. Lett. **104B**, 199 (1981).
[18] A. P. Zhitnitskii, Possible suppression of axion-hadron interactions, Sov. J. Nucl. Phys. **31**, 260 (1980).
[19] S. Knirck, A. J. Millar, and C. A. O'Hare, J. Redondo, and F. D. Steffen, Directional axion detection, J. Cosmol. Astropart. Phys. 11 (2018) 051.
[20] C. Kittel, *Introduction to Solid State Physics*, 8th ed. (Wiley, Hoboken, NJ, 2005).
[21] M. Deeter, A. Rose, and G. Day, Fast, sensitive magnetic-field sensors based on the faraday effect in YIG, J. Lightwave Technol. **8**, 1838 (1990).
[22] R. Hisatomi, A. Osada, Y. Tabuchi, T. Ishikawa, A. Noguchi, R. Yamazaki, K. Usami, and Y. Nakamura, Bidirectional conversion between microwave and light via ferromagnetic magnons, Phys. Rev. B **93**, 174427 (2016).
[23] J. F. Dillon, H. Kamimura, and J. P. Remeika, Magneto-optical studies of chromium tribromide, J. Appl. Phys. **34**, 1240 (1963).
[24] H. Hemmati, P. Bootpakdeetam, and R. Magnusson, Metamaterial polarizer providing principally unlimited extinction, Opt. Lett. **44**, 5630 (2019).
[25] J. H. W. G. den Boer, G. M. W. Kroesen, W. de Zeeuw, and F. J. de Hoog, Improved polarizer in the infrared: Two wire-grid polarizers in tandem, Opt. Lett. **20**, 800 (1995).
[26] M. Fox, *Quantum Optics: An Introduction* (Oxford University Press, New York, 2006).
[27] F. Ceccarelli, G. Acconcia, A. Gulinatti, M. Ghioni, I. Rech, and R. Osellame, Recent advances and future perspectives of single-photon avalanche diodes for quantum photonics applications, Adv. Quantum Technol. **4**, 2000102 (2021).
[28] I. Esmaeil Zadeh, J. Chang, J. W. N. Los, S. Gyger, A. W. Elshaari, S. Steinhauer, S. N. Dorenbos, and V. Zwiller, Superconducting nanowire single-photon detectors: A perspective on evolution, state-of-the-art, future developments, and applications, Appl. Phys. Lett. **118**, 190502 (2021).
[29] L. Schweickert, K. D. Jöns, K. D. Zeuner, S. F. Covre da Silva, H. Huang, T. Lettner, M. Reindl, J. Zichi, R. Trotta, A. Rastelli, and V. Zwiller, On-demand generation of background-free single photons from a solid-state source, Appl. Phys. Lett. **112**, 093106 (2018).
[30] E. Lage, L. Beran, A. U. Quindeau, L. Ohnoutek, M. Kucera, R. Antos, S. R. Sani, G. F. Dionne, M. Veis, and C. A. Ross, Temperature-dependent faraday rotation and magnetization reorientation in cerium-substituted yttrium iron garnet thin films, APL Mater. **5**, 036104 (2017).
[31] S. Higuchi, Y. Furukawa, S. Takekawa, O. Kamada, K. Kitamura, and K. Uyeda, Magnetooptical properties of cerium-substituted yttrium iron garnet single crystals for magnetic-field sensor, Sens. Actuator A Phys. **105**, 293 (2003).
[32] D. Lachance-Quirion, Y. Tabuchi, A. Gloppe, K. Usami, and Y. Nakamura, Hybrid quantum systems based on magnonics, Appl. Phys. Express **12**, 070101 (2019).
[33] A. T. M. A. Rahman, Large spatial schrödinger cat state using a levitated ferrimagnetic nanoparticle, New J. Phys. **21**, 113011 (2019).
[34] S. Higuchi, Y. Furukawa, S. Takekawa, O. Kamada, and K. Kitamura, Magneto-optical properties of cerium-substituted yttrium iron garnet single crystals grown by traveling solvent floating zone method, Jpn. J. Appl. Phys. **38**, 4122 (1999).
[35] Rio GRANDE, https://rio-lasers.com/.

[36] F. Meylahn, N. Knust, and B. Willke, Stabilized laser system at 1550 nm wavelength for future gravitational-wave detectors, Phys. Rev. D **105**, 122004 (2022).

[37] M. Callon *et al.*, Biomolecular solid-state NMR spectroscopy at 1200 MHz: The gain in resolution, J. Biomol. NMR **75**, 255 (2021).

[38] S. Hahn, K. Kim, K. Kim, X. Hu, T. Painter, I. Dixon, S. Kim, K. R. Bhattarai, S. Noguchi, J. Jaroszynski, and D. C. Larbalestier, 45.5-tesla direct-current magnetic field generated with a high-temperature superconducting magnet, Nature (London) **570**, 496 (2019).

[39] J. Miller, The NHMFL 45-T hybrid magnet system: Past, present, and future, IEEE Trans. Appl. Supercond. **13**, 1385 (2003).

[40] G. Rempe, R. J. Thompson, H. J. Kimble, and R. Lalezari, Measurement of ultralow losses in an optical interferometer, Opt. Lett. **17**, 363 (1992).

[41] E. G. Spencer, R. C. LeCraw, and R. C. Linares, Low-temperature ferromagnetic relaxation in yttrium iron garnet, Phys. Rev. **123**, 1937 (1961).

[42] J. Aasi, M. v. d. Sluys, J. Zweizig *et al.*, Enhanced sensitivity of the ligo gravitational wave detector by using squeezed states of light, Nat. Photonics **7**, 613 (2013).

[43] R. Hisatomi, A. Noguchi, R. Yamazaki, Y. Nakata, A. Gloppe, Y. Nakamura, and K. Usami, Helicity-Changing Brillouin Light Scattering by Magnons in a Ferromagnetic Crystal, Phys. Rev. Lett. **123**, 207401 (2019).

[44] D. J. E. Marsh, K. C. Fong, E. W. Lentz, L. Šmejkal, and M. N. Ali, Proposal to Detect Dark Matter Using Axionic Topological Antiferromagnets, Phys. Rev. Lett. **123**, 121601 (2019).